Orientation Dependence of Grain-Boundary Critical Currents in $YBa_2Cu_3O_{7-\delta}$ Bicrystals

D. Dimos, P. Chaudhari, J. Mannhart, and F. K. LeGoues
Thomas J. Watson Research Center, IBM Research Division, Yorktown Heights, New York, 10598
(Received 4 May 1988)

The critical current densities across grain boundaries have been measured as a function of misorientation angle in the basal plane of bicrystals of $YBa_2Cu_3O_{7-\delta}$. For small misorientation angles, the ratio of the grain-boundary critical current density to the bulk critical current density is roughly proportional to the inverse of the misorientation angle; for large angles, this ratio saturates to a value of about $\frac{1}{50}$. These results imply that achieving a high degree of texture both normal to and within the basal plane is important for the obtaining of very high critical currents in pure polycrystalline samples.

PACS numbers: 74.60.Jg, 74.70.Vy

The low critical current densities of polycrystalline $YBa_2Cu_3O_{7-\delta}$, as compared to typical values for single crystals and epitaxial thin films [$J_c \simeq (1\text{-}10)\times 10^6$ A/cm^2 at 4.2 K],[1,2] have generally been attributed to a combination of critical-current anisotropy and poor superconducting coupling across grain boundaries.[3,4] By measuring the superconducting properties of individual grain boundaries, we have recently presented direct evidence that the critical current density across a grain boundary is always significantly less than that of either adjacent grain.[5] Although these measurements directly demonstrated the weak coupling, they did not address the relationship between the grain misorientations and the critical current densities across the grain boundaries. The relationship is important since a number of investigators have assumed that by texturing polycrystalline samples such that the c axes of the grains are aligned, very high critical current densities could be obtained. We have, therefore, measured the critical current density between two grains whose c axes were almost parallel but which are rotated about the c axis with respect to each other.

The bicrystals of $YBa_2Cu_3O_{7-\delta}$ were prepared by epitaxial growth of thin films on $SrTiO_3$ bicrystals with nominally symmetric [100] tilt boundaries. The midpoint transition temperatures of the superconducting films were 86–88 K while the transition widths were 3–6 K. The geometry of the substrates, which were fabricated by sintering two oriented single crystals of $SrTiO_3$, is illustrated in the schematic diagram in Fig. 1. The acute angle, θ, between (100) planes in the two $SrTiO_3$ crystals defines the misorientation angle in the basal plane of the thin-film bicrystal. Alignment errors also caused the cube axes of the two crystals which were normal to the plane of the film (the [001] vectors in Fig. 1) to be misaligned by an angle ϕ in a plane normal to the grain-boundary plane and by a negligible angle ($\leq 1°$) in a plane parallel to the grain-boundary plane. Consequently, the c axes of the two $YBa_2Cu_3O_{7-\delta}$ grains, which are approximately normal to the plane of the film, are misaligned by the angle ϕ, which introduces a second component of tilt at the grain boundary. All of the misorientation angles, which were determined by back Laue x-ray diffraction, were measured to $\pm \frac{1}{2}°$.

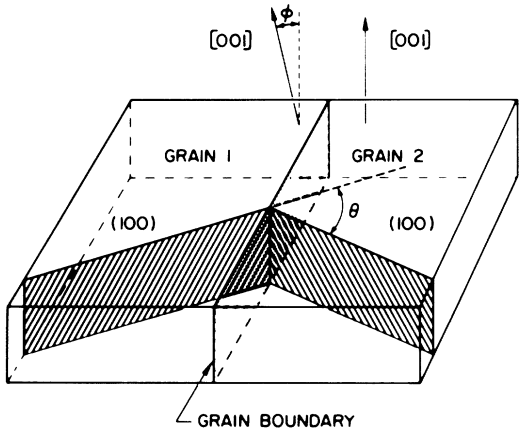

FIG. 1. Schematic diagram showing the important crystallography of the $SrTiO_3$ bicrystals which were used as substrates for the thin-film deposition.

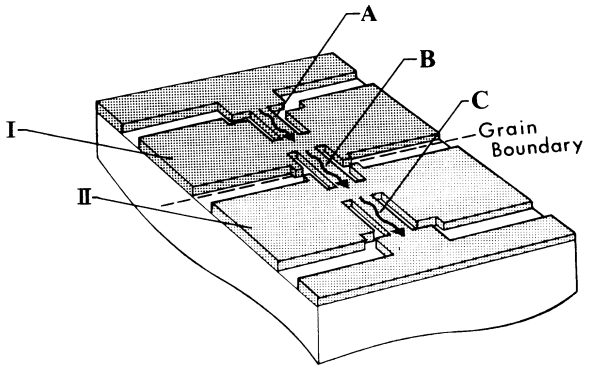

FIG. 2. Schematic diagram of the patterned film showing the two grains (regions I and II) and the three narrow lines. Lines A and C are contained entirely within grains I and II, respectively, while line B straddles the grain boundary.

TABLE I. Critical current density (10^3 A/cm^2) at 4.2–5 K.

θ (ϕ)	Grain 1	Grain 2	Grain Boundary
0° (3°)	7140	8000	4000
3° (7°)	5900	5300	1400
4° (4°)	270	220	73
5° (9°)	6000	5700	560
7° (4°)	140	180	40
10° (4°)	7800	8000	410
10° (4°)	7000	6100	240
12.5° (2°)	3800	3400	160
22° (2°)	800	260	11
35.5° (4°)	1350	1400	25

Narrow lines, approximately 10 μm wide, were patterned into two single-grain regions and across the grain boundary, as shown in Fig. 2, with use of a previously described excimer-laser fabrication technique.[6] Electrical contacts, made directly to the film with aluminum wire bonds, were Ohmic with resistances of 20–50 Ω. The current-voltage characteristics of each line were measured with a four-point technique. The critical current densities were obtained by dividing the maximum zero-voltage current by the cross-sectional area of the patterned lines or by the macroscopic area of grain boundary contained within the line when the grain-boundary plane was not perpendicular to the direction of the line. Table I lists the critical current densities determined for both grains and the grain boundary for each bicrystal at 4.2–5 K. The tilt angle in the basal plane, θ, and the orthogonal tilt angle, ϕ, are given for each sample. Since the critical current density for the line containing the grain boundary was always less than for either grain, the lower J_c was attributed to the grain-boundary region. The critical current density across the $\theta=0°$ grain boundary was also reduced by about a factor of 2 from the bulk value. This reduction in J_c may be entirely due to misorientations caused by the nonzero value of ϕ or to the fact that θ may not be exactly zero. In addition, porosity present at the sintered grain boundaries of the $SrTiO_3$ substrates causes imperfections in the film that could also reduce the grain-boundary critical current densities.

The ratio of the grain-boundary critical current density to the average value of the grain critical current density, J_c^{gb}/J_c^G, shows a strong correlation with the tilt angle θ, but shows little correlation with the tilt angle ϕ. Consequently, this ratio is plotted as a function of the tilt angle θ in Fig. 3. The critical-current ratio is plotted on a logarithmic scale which vividly shows that this ratio varies by almost 2 orders of magnitude over the range $\theta=0°$–$35°$ and that J_c^{gb}/J_c^G is approximately proportional to $1/\theta$, for small θ. Furthermore, this ratio reaches a saturation value of about $\frac{1}{50}$ at a tilt angle of about 20°. The scatter in the data of Fig. 4 could be attributed to inaccuracies in the determination of the cross-sectional areas of the superconducting lines or possibly to compositional inhomogeneities in the films. Ohmic heating at the wire-bonded contacts did not affect the measurements as indicated by the fact that immersion of the samples in liquid He did not change the measured critical currents. Furthermore, the way in which the grain-boundary structure affects its critical current density appears to be independent of film quality, since the J_c ratios obtained by use of films with low critical current

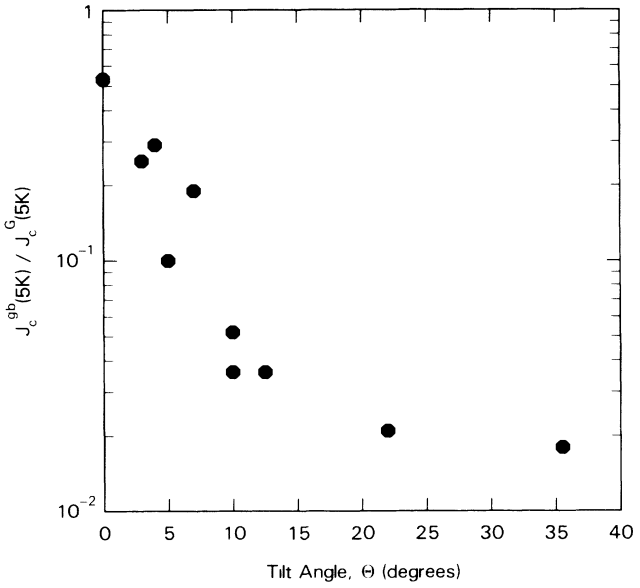

FIG. 3. Plot of the ratio of the grain-boundary critical current density to the average value of the critical current density in the two grains at 4.2–5 K vs the misorientation angle in the basal plane.

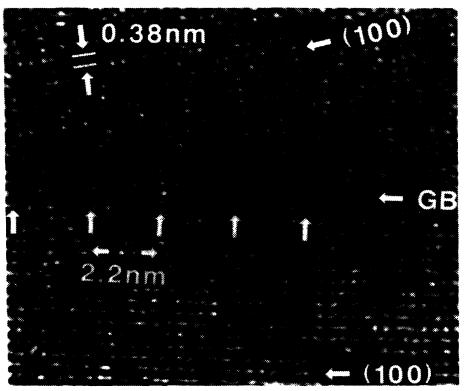

FIG. 4. Lattice fringe image of a $\theta=10°$ grain boundary viewed normal to the grain-boundary plane. The location of the grain-boundary dislocations, which correspond to the termination points of the (100) lattice fringes at the grain-boundary plane, are shown by the arrows. These dislocations have a spacing of 2.2 nm.

densities ($J_c^G < 5\times10^5$ A/cm^2) are consistent with the results obtained with high-J_c films.

Although the data in Table I and Fig. 4 are for liquid-He temperatures, the temperature dependences of the critical current densities for the grains and the grain boundaries are essentially identical. Therefore, the J_c ratios and the dependence of J_c^{gb}/J_c^G on the misorientation angle are roughly independent of temperature. It should also be noted that the critical current densities for grains and grain boundaries at 77 K had a value about 10% of that found at 4.2 K.

To relate the superconducting properties to the structure of the grain boundary, we have studied some of the grain boundaries by transmission electron microscopy. Figure 4 is a typical example of a lattice fringe image of one of the grain boundaries viewed normal to the grain-boundary plane; in this case, $\theta=10°$. The continuity of the lattice fringes in both grains up to the grain-boundary plane indicates that the boundary is clean (i.e., free of grain-boundary phases). The contrast of this image, which is poor because of the thickness of the transmission electron microscopy foil in the region of interest, has been enhanced by a Fourier filtering process. The dislocations that accommodate the misorientation angle θ are seen as the termination points of the lattice fringes at the grain-boundary plane. These dislocations have a spacing of 22 Å, which is consistent with a value for the Burgers vector of about 3.8 Å as observed previously in tilt boundaries of this type.[7] However, these grain boundaries are typically neither exactly straight nor exactly symmetric, as is evident in Fig. 4, so that more than one type of grain-boundary dislocation may be present. The dislocation spacing, however, remains roughly proportional to the inverse of the misorientation angle. With increasing misorientation angle, the dislocation cores eventually overlap so that the grain boundary is no longer composed of discrete dislocations.

Although the absence of grain-boundary phases has been confirmed by electron microscopy, these observations do not eliminate the possibility of compositional variations at the grain boundaries. In particular, rapid grain-boundary diffusion of Sr and Ti could lead to an enhancement in their concentrations at the boundary which might affect J_c^{gb}, since both elements are known to depress T_c.[8] To address this possibility, the distribution of Sr and Ti in the film as a function of depth was monitored with use of secondary-ion mass spectroscopy in a field-imaging mode. The concentrations of Sr and Ti in the vicinity of the grain boundary were not distinguishably different from their concentrations in the bulk of the film, except close to the film-substrate interface where some enhancement associated with the grain boundary was observed. This result is quite reasonable since bulk diffusion kinetics is expected to dominate the interdiffusion process at the relatively high tempertures ($\simeq$950 °C) used to anneal the films. Rapid volume diffusion is also suggested by the observation that the Sr and Ti concentrations are essentially uniform throughout the thickness of the film. In addition, the critical current densities of epitaxial films do not seem especially sensitive to changes in Sr and Ti content, since an extended anneal (120 min vs min at 925 °C), which caused a reduction in the zero-resistance T_c of about 3 K, resulted in only a modest decrease in J_c ($\simeq$50%). Consequently, we believe that the systematic reduction in J_c^{gb}/J_c^G with increasing misorientation is a result of changes in grain-boundary structure and that the trend shown in Fig. 3 reflects an intrinsic property of tilt boundaries in these materials.

Since both the ratio J_c^{gb}/J_c^G and the spacing between grain-boundary dislocations are roughly proportional to $1/\theta$, for small θ, the dislocation arrangement in the grain boundary is concluded to be the important factor in the determination of the critical current densities across these grain boundaries. This conclusion is also consistent with the fact that the J_c ratio appears to saturate at an angle roughly equal to that at which the dislocations are expected to overlap. The dislocation array could reduce the grain-boundary critical current density relative to its value in the bulk by acting either as a partial barrier to the flow of supercurrent or as an easy path for flux flow. Both mechanisms rely on the assumption that the superconducting order parameter is depressed in the neighborhood of the boundary. Such a depression can arise from the structural disorder at dislocation cores and from distortions caused by the strain field of the grain boundary.

If the order parameter is depressed at each dislocation core, the area of the grain boundary through which good superconducting coupling occurs will be less than the actual area of the boundary. The good area of the boundary will depend on the spacing between dislocations and on the area of the poor superconducting region surrounding each dislocation. If J_c^{gb} is proportional to the good area of the grain boundary, the grain-boundary critical current density should scale with the bulk critical current density, J_c^G, as observed. The large decrease in J_c^{gb} at small angles, where the dislocation spacing is much greater than the core diameter ($d \gg r_0$), can only be accounted for if the superconducting coupling is severely degraded over an area with a radius much greater than the core radius, where $r_0 \simeq b$. This situation is realistic since the length scale over which the order parameter can change from its depressed value to its bulk value is the coherence length in the basal plane, which has a value of about 20–30 Å. However, this reasoning implies that J_c^{gb}/J_c^G should approach a minimum value at an angle smaller than that at which the dislocation cores begin to overlap.

Alternatively, the angular dependence of J_c^{gb} could be primarily determined by the effect of the dislocation structure of flux pinning within the grain boundary. If flux flow is easier along the grain boundary than in the

bulk, the grain-boundary dislocations have a lower pinning energy than the bulk. The primary effect of the grain-boundary dislocations may be to distort the flux vortices so that they are elongated in the grain-boundary plane where the order parameter is depressed. If the resistance to flux motion is determined by intrinsic pinning in the undistorted regions of the lattice, J_c^{gb} will be roughly proportional to the bulk critical current, as we find, and scale inversely with the elongation of the vortices in the boundary plane. The strong dependence of J_c^{gb}/J_c^G on misorientation angle implies that the distortion of the vortices is determined by the spacing between grain-boundary dislocations. The effect of the grain-boundary structure on vortex elongation, and thus the J_c ratio, would saturate when the dislocation cores begin to overlap, which should occur at about the observed saturation angle of $\theta \simeq 20°$ (i.e., $d \simeq 2r_0$).

The results of this study have important consequences to the problem of attaining high critical current densities in polycrystalline samples. While it has been shown that substantial increases in critical current density can be obtained by the production of highly textured microstructures in which the c axes of the grains are nearly parallel, the largest J_c's presently being achieved at 77 K are about 2 orders of magnitude lower than for the best epitaxial films at 77 K.[9] In fact, even if samples can be fabricated with almost perfect c-axis alignment, misorientations in the basal planes between adjacent grains will limit the critical current density. Our data suggest that, by the production of a high degree of alignment both normal to and within the basal plane, it should be possible to achieve bulk critical current densities that are at least an order of magnitude higher than those being obtained presently.

The authors are indebted to G. J. Scilla for performing the secondary-ion mass-spectroscopy analysis, W. Krakow for the Fourier filtering of the electron micrograph, and M. M. Oprysko for use of the excimer laser. We also want to thank T. M. Shaw, D. R. Clarke, C. C. Tsuei, and J. Chi for helpful discussions, and J. Lacey, P. R. Duncombe, and J. Berosh for technical assistance.

[1]T. R. Dinger, T. K. Worthington, W. J. Gallagher, and R. L. Sandstrom, Phys. Rev. Lett. **58**, 2687 (1987).

[2]P. Chaudhari, R. H. Koch, R. B. Laibowitz, T. R. McGuire, and R. J. Gambino, Phys. Rev. Lett. **58**, 2684 (1987).

[3]P. Chaudhari, F. LeGoues, and A. Segumuller, Science **238**, 342 (1987).

[4]R. A. Campo, J. E. Evetts, B. A. Glowacki, S. B. Newcomb, R. E. Somekh, and W. M. Stobbs, Nature (London) **329**, 229 (1987).

[5]P. Chaudhari, J. Mannhart, D. Dimos, C. C. Tsuei, J. Chi, M. M. Oprysko, and M. Scheuermann, Phys. Rev. Lett. **60**, 1653 (1988).

[6]J. Mannhart, M. Scheuermann, C. C. Tsuei, M. M. Oprysko, C. C. Chi, C. P. Umbach, R. H. Koch, and C. Miller, Appl. Phys. Lett. **52**, 1271 (1988).

[7]M. F. Chisholm and D. A. Smith, Philos. Mag. A (to be published).

[8]M. F. Yan, W. W. Rhodes, and P. K. Gallagher, J. Appl. Phys. **63**, 821 (1988).

[9]S. Jin, T. H. Tiefel, R. C. Sherwood, M. E. Davis, R. B. van Dover, G. W. Kammlott, R. A. Fastnacht, and H. D. Keith, Appl. Phys. Lett. **52**, 2074 (1988).

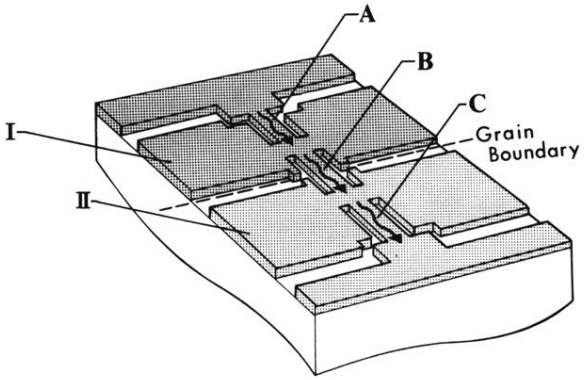

FIG. 2. Schematic diagram of the patterned film showing the two grains (regions I and II) and the three narrow lines. Lines A and C are contained entirely within grains I and II, respectively, while line B straddles the grain boundary.

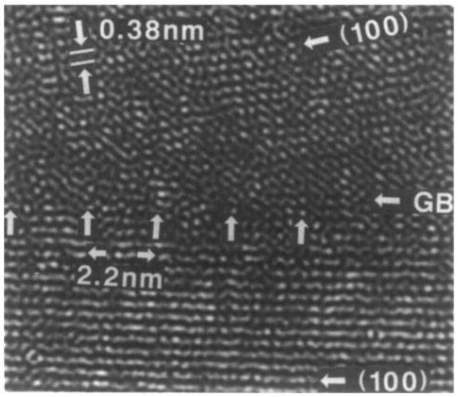

FIG. 4. Lattice fringe image of a $\theta = 10°$ grain boundary viewed normal to the grain-boundary plane. The location of the grain-boundary dislocations, which correspond to the termination points of the (100) lattice fringes at the grain-boundary plane, are shown by the arrows. These dislocations have a spacing of 2.2 nm.